

Dendritic and uniform flux jumps in superconducting films

D. V. Denisov,^{1,2} A. L. Rakhmanov,³ D. V. Shantsev,^{1,2} Y. M. Galperin,^{1,2,4} and T. H. Johansen^{1,*}

¹*Department of Physics and Center for Advanced Materials and Nanotechnology, University of Oslo, P.O. Box 1048 Blindern, 0316 Oslo, Norway*

²*A. F. Ioffe Physico-Technical Institute, Polytekhnicheskaya 26, St. Petersburg 194021, Russia*

³*Institute for Theoretical and Applied Electrodynamics, Izhorskaya 13/19, Moscow 125412, Russia*

⁴*Argonne National Laboratory, 9700 South Cass Avenue, Argonne, Illinois 60439, USA*

(Received 7 October 2005; published 13 January 2006; publisher error corrected 15 February 2006)

Recent theoretical analysis of spatially-nonuniform modes of the thermomagnetic instability in superconductors [Phys. Rev. B **70**, 224502 (2004)] is generalized to the case of a thin film in a perpendicular applied field. We solve the thermal diffusion and Maxwell equations taking into account nonlocal electrodynamics in the film and its thermal coupling to the substrate. The instability is found to develop in a nonuniform, fingering pattern if the background electric field, E , is high and the heat transfer coefficient to the substrate, h_0 , is small. Otherwise, the instability develops in a uniform manner. We find the threshold magnetic field, $H_{\text{fing}}(E, h_0)$, the characteristic finger width, and the instability buildup time. Thin films are found to be much more unstable than bulk superconductors, and have a stronger tendency for formation of fingering (dendritic) pattern.

DOI: [10.1103/PhysRevB.73.014512](https://doi.org/10.1103/PhysRevB.73.014512)

PACS number(s): 74.25.Qt, 74.25.Ha, 68.60.Dv

I. INTRODUCTION

The thermomagnetic instability or flux jumping is commonly observed at low temperatures in type-II superconductors with strong pinning.^{1–4} The instability arises for two fundamental reasons: (i) motion of magnetic flux releases energy, and hence increases the local temperature; (ii) the temperature rise decreases flux pinning, and hence facilitates the further flux motion. This positive feedback can result in thermal runaways and global flux redistributions jeopardizing superconducting devices. The conventional theory of the thermomagnetic instability^{1,2} considers only “uniform” flux jumps, where the flux front is smooth and essentially straight. This picture is true for many experimental conditions, however, far from all. Numerous magneto-optical studies have recently revealed that the thermomagnetic instability in superconductors can result in strongly branched dendritic flux patterns.^{5–19}

In a recent paper we examined the problem of flux pattern formation in the *slab* geometry.²⁰ Experimentally, however, the dendritic flux patterns are mostly observed in *thin film* superconductors placed in a perpendicular magnetic field. An analysis of this perpendicular geometry was recently published by Aranson *et al.*²¹ Here we present a more exact and complete picture of the dendritic instability and analyze the criteria of its realization.

In the following we restrict ourselves to a conventional linear analysis^{1,2,22} of the instability and consider the space-time development of small perturbations in the electric field, E , and temperature, T . In contrast to the slab case,²⁰ the heat transfer from the superconductor to a substrate as well as the nonlocal electrodynamics in thin films are taken into account. Consequently, the results depend significantly on the heat transfer rate, h_0 , as well as on the film thickness, d . Our main result is that the instability in the form of narrow fingers perpendicular to the background field, \mathbf{E} , occurs much easier in thin films than in slabs and bulk samples, and the corresponding threshold field, E_c , is found to be proportional to the film thickness, d .

II. MODEL AND BASIC EQUATIONS

Consider the perpendicular geometry shown in Fig. 1, with a thin superconducting strip placed in a transverse magnetic field, \mathbf{H} . The strip is infinite along the y axis, and occupies the space from $-d/2$ to $d/2$ in the z direction and from 0 to $2w$ in the x direction. It is assumed that $d \ll w$. In the unperturbed state the screening current flows along the y axis. The distributions of the current density, \mathbf{j} , and magnetic induction, \mathbf{B} , in the flux penetrated region $0 < x < \ell$ are determined by the Maxwell equation

$$\text{curl } \mathbf{B} = \mu_0 \mathbf{j}, \quad (1)$$

where the common approximation $\mathbf{B} = \mu_0 \mathbf{H}$ is used. To find the electric field and the temperature we use another Maxwell equation together with the equation for thermal diffusion

$$\text{curl } \mathbf{E} = -\partial \mathbf{B} / \partial t, \quad (2)$$

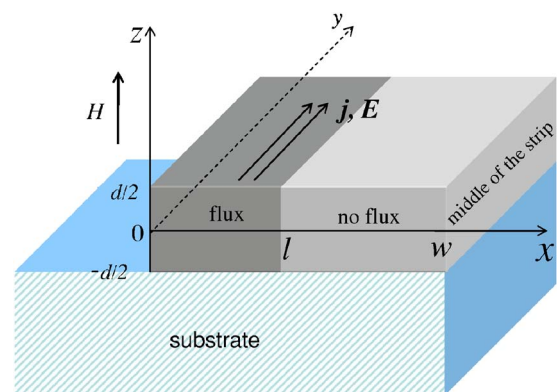


FIG. 1. (Color online) A superconductor strip on a substrate (only the left half is shown). The dark gray area is the flux-penetrated region.

$$C(\partial T/\partial t) = \kappa \nabla^2 T + \mathbf{j} \cdot \mathbf{E}. \quad (3)$$

Here C and κ are the specific heat and thermal conductivity, respectively.

Equations (1)–(3) should be supplemented by a current-voltage relation $j = j(E, B, T)$. For simplicity we assume a current-voltage curve of the form

$$\mathbf{j} = j_c(T)g(E)(\mathbf{E}/E). \quad (4)$$

A strong nonlinearity of the function $g(E)$ leads to formation of a quasistatic critical state with $j \approx j_c(T)$, where j_c is the critical current density.²³ We neglect any B dependence of j_c , i.e., adopt the Bean model. The exact form of $g(E)$ is not crucially important, the only issue is that it represents a very steep $E(j)$ curve having a large logarithmic derivative

$$n(E) \equiv \partial \ln E / \partial \ln j \approx j_c / \sigma E \gg 1. \quad (5)$$

Here σ is the differential electrical conductivity, $\sigma(E) \equiv \partial j / \partial E$. The parameter n generalizes the exponent in the frequently used power-law relation $E \propto j^n$ with n independent of E .

The key dimensionless parameter of the model is the ratio of thermal and magnetic diffusion coefficients,¹

$$\tau \equiv \mu_0 \kappa \sigma / C. \quad (6)$$

The smaller τ is, the slower heat diffuses from the perturbation region into the surrounding areas. Hence, one can expect that for smaller τ : (i) the superconductor is more unstable, and (ii) the formation of instability-induced nonuniform structures is more favorable.

In the following we assume that the strip is thinner than the London penetration depth, λ_L , and at the same time much wider than the effective penetration length, $\lambda_{\text{eff}} = \lambda_L^2 / d$

$$d \leq \lambda_L \ll \sqrt{dw}.$$

The stationary current and field distributions in a thin strip under such conditions were calculated by several authors,^{24–26} finding that the flux penetration depth, ℓ , is related to the applied field by the expression

$$\ell / w = \pi^2 H^2 / 2 d^2 j_c^2. \quad (7)$$

Here it is assumed that the penetration is shallow, or more precisely that $\lambda_{\text{eff}} \ll \ell \ll w$.

III. PERTURBATION ANALYSIS

A. Linearized dimensionless equations

We seek solutions of Eqs. (1)–(4) in the form

$$T + \delta T(x, y, z, t), \quad \mathbf{E} + \delta \mathbf{E}(x, y, z, t), \quad \mathbf{j} + \delta \mathbf{j}(x, y, z, t),$$

where T , \mathbf{E} , and \mathbf{j} are background values. The background electric field may be created, e.g., by ramping the external magnetic field, and for simplicity we assume it to be coordinate independent. Allowing for such a dependence would only lead to insignificant numerical corrections, as discussed in Ref. 20. Similarly, we will assume a uniform background temperature.

Whereas it follows from symmetry considerations that $E_x = 0$, both components of the perturbation, $\delta \mathbf{E}$, will in general not vanish. Linearizing the current-voltage relation, Eq. (4) one obtains

$$\delta \mathbf{j} = \left(\frac{\partial j_c}{\partial T} \delta T + \sigma \delta E_y \right) \frac{\mathbf{E}}{E} + j_c \frac{\delta \mathbf{E}_x}{E}. \quad (8)$$

We shall seek perturbations in the form

$$\delta T = T^* \theta \exp(\lambda t / t_0 + ik_x \xi + ik_y \eta),$$

$$\delta E_{x,y} = E \varepsilon_{x,y} \exp(\lambda t / t_0 + ik_x \xi + ik_y \eta),$$

$$\delta j_{x,y} = j_c i_{x,y} \exp(\lambda t / t_0 + ik_x \xi + ik_y \eta), \quad (9)$$

where θ , ε , and i are z -dependent dimensionless Fourier amplitudes. The coordinates are normalized to the adiabatic length $a = \sqrt{CT^* / \mu_0 j_c^2}$ where $T^* = -(\partial \ln j_c / \partial T)^{-1}$ is the characteristic scale of the temperature dependence of j_c , so that $\xi = x/a$, $\eta = y/a$, $\zeta = z/a$. The time is normalized to $t_0 = \sigma CT^* / j_c^2 = \mu_0 \sigma a^2$, which is the magnetic diffusion time for the length a . $\text{Re } \lambda$ is the dimensionless instability increment, which when positive indicates exponential growth of the perturbation.

We can now use the formulas (9) to rewrite the basic equations in dimensionless variables. From Eq. (8) one finds for the components of the current density perturbation \mathbf{i}

$$i_x = \varepsilon_x, \quad i_y = -\theta + n^{-1} \varepsilon_y. \quad (10)$$

Combining the Maxwell equations (1) and (2), and the thermal diffusion equation (3) yields

$$\mathbf{k} \times [\mathbf{k} \times \boldsymbol{\varepsilon}] = \lambda n \mathbf{i}, \quad (11)$$

$$\lambda \theta = \tau \left(-k_y^2 \theta + \frac{\partial^2 \theta}{\partial \xi^2} \right) + (i_y + \varepsilon_y) / n. \quad (12)$$

Magneto-optical imaging shows that flux patterns produced by the dendritic instability^{5–19} are characterized by having $k_y \gg k_x$. Therefore, we have neglected the heat flow along the x direction compared to that along the y direction. Later we will check the consistency of this assumption by showing that indeed the fastest growing perturbation has $k_y \gg k_x$.

B. Boundary conditions

We assume that heat exchange between the superconducting film and its environment follows the Newton cooling law. For simplicity we let the boundary condition, $\kappa \nabla(T + \delta T) = -h_0(T + \delta T - T_0)$, apply to both film surfaces. Here T_0 and h_0 are the effective environment temperature and heat transfer coefficient, respectively. Equations (12) and (10) can now be integrated over the film thickness to yield

$$\theta = \frac{(1 + n^{-1}) \varepsilon_y}{n \lambda + n \tau (k_y^2 + h) + 1},$$

where

$$h = 2h_0 a^2 / \kappa d. \quad (13)$$

In the remaining part of the paper we let θ , ε , and \mathbf{i} denote perturbations averaged over the film thickness.

We seek a solution of the electrodynamic equations in the flux penetrated region, $0 \leq \xi \leq \ell/a$. At the film edge, $\xi=0$, one has $\delta j_x=0$ and, consequently, $\delta E_x=0$. In the Meissner state both the electric field and heat dissipation are absent, so that $\delta E_y = \delta T = \delta j_y = 0$ at the flux front, $\xi = \ell/a$. Thus, the Fourier expansions for the x and y components of electric field perturbation will contain only $\sin(k_x \xi)$ and $\cos(k_x \xi)$, respectively. Then the boundary conditions are satisfied for

$$k_x = (\pi a / 2\ell)(2s + 1), \quad s = 0, 1, 2, \dots$$

Since ℓ depends on the magnetic field, the values of k_x are also magnetic field dependent.

Now we can integrate Eq. (11) over the film thickness and employ the symmetry of the electrodynamic problem with respect to the plane $z=0$. It yields

$$\begin{aligned} -ik_y(k_x \varepsilon_y + ik_y \varepsilon_x) - \frac{2a}{d} \varepsilon'_x &= -\lambda n \varepsilon_x, \\ -k_x(k_x \varepsilon_y + ik_y \varepsilon_x) + \frac{2a}{d} \varepsilon'_y &= -\lambda n f(\lambda, k_y) \varepsilon_y. \end{aligned} \quad (14)$$

We have here introduced the function

$$f(\lambda, k_y) \equiv \frac{i_y}{\varepsilon_y n} \frac{1}{n\lambda + n\tau(k_y^2 + h) + 1}.$$

Note that the equation for the z component of the field is satisfied automatically. The derivatives $\varepsilon'_{x,y}$ with respect to ζ are taken at the film surface, $\zeta = d/2a$. To calculate them, one needs the electric field distribution outside the superconductor, where the flux density is given by the Bio-Savart law

$$\mathbf{B}(\mathbf{r}) = \mu_0 \mathbf{H} + \frac{\mu_0}{4\pi} \int d^3 \mathbf{r}' \frac{\mathbf{j} \times (\mathbf{r} - \mathbf{r}')}{|\mathbf{r} - \mathbf{r}'|^3}.$$

The perturbation of flux density is then

$$\delta B_{x,y} = \pm \mu_0 \zeta d \int_0^{\ell/a} d\xi' \int_{-\infty}^{\infty} d\eta' G(\xi - \xi', \eta - \eta') \delta j_{y,x},$$

$$G(\xi, \eta) = \frac{1}{4\pi[\xi^2 + \eta^2 + (d/2a)^2]^{3/2}}.$$

Here we have approximated the average over ζ' substituting $\zeta' = 0$. In this way we omit only terms of the order of $(d/a)^2 \ll 1$. The integration over ξ' should, in principle, cover also the Meissner region, $\xi' > \ell/a$. Though the flux density there remains zero during the development of perturbation, the Meissner current will be perturbed due to the nonlocal current-field relation. However the kernel $G(\xi, \eta)$ decays very fast at distances larger than d/a and therefore the Meissner current perturbation produces only insignificant numerical corrections.

The perturbation of the magnetic field can be related to that of the electrical field by Eq. (2), which can be rewritten as

$$\delta E'_{x,y} / E = \mp \lambda n \delta B_{y,x} / \mu_0 a j_c. \quad (15)$$

Due to continuity of the magnetic field tangential components Eq. (15) is also valid at the film surface, $\zeta = d/2a$. Thus it can be substituted into Eqs. (14). The Fourier components of the kernel function $G(\xi, \eta)$ with respect to η can be calculated directly yielding

$$G(\xi, k_y) = \frac{k_y a K_1[k_y \sqrt{\xi^2 + (d/2a)^2}]}{2\pi \ell \sqrt{\xi^2 + (d/2a)^2}}, \quad (16)$$

where K_1 is the modified Bessel function of the second kind.

The above Fourier expansions in $\cos(k_x \xi)$ and $\sin(k_x \xi)$ correspond to the finite interval $-2\ell/a < \xi < 2\ell/a$. Therefore we should continue $\varepsilon_{x,y}$ from $0 < \xi < \ell/a$ to this interval and then introduce G_x and G_y as analytical continuations of $G(\xi - \xi', k_y)$ having the same symmetry as ε_x and ε_y , respectively (see Ref. 27 for details). All this allows us to rewrite the set (14) as

$$-ik_x k_y \varepsilon_y + (k_y^2 + \lambda n) \varepsilon_x = (d/2a) \lambda n \sum_{k'_x} G_x(k_x, k'_x, k_y) \varepsilon_x(k'_x), \quad (17)$$

$$(k_x^2 + \lambda n f) \varepsilon_y + ik_x k_y \varepsilon_x = (d/2a) \lambda n f \sum_{k'_x} G_y(k_x, k'_x, k_y) \varepsilon_y(k'_x), \quad (18)$$

$$\begin{aligned} \left\{ \begin{array}{l} G_x(k_x, k'_x, k_y) \\ G_y(k_x, k'_x, k_y) \end{array} \right\} &= 4 \int_0^{\ell/a} d\xi \int_0^{\ell/a} d\xi' G(\xi - \xi', k_y) \\ &\times \left\{ \begin{array}{l} \sin(k_x \xi) \sin(k'_x \xi') \\ \cos(k_x \xi) \cos(k'_x \xi') \end{array} \right\}. \end{aligned} \quad (19)$$

We are interested only in the specific case of a very thin strip

$$\alpha = d/2\ell \ll 1. \quad (20)$$

One can then find analytical expressions for the kernel, and it turns out that only its diagonal part, $k_x = k'_x$, is important.

In this paper we present analytical expressions up to the first order in α , while the plots are calculated up to the second order. The second-order analytical expressions can be found in Ref. 27. The kernel (19) can be written as

$$G_{x,y}(k_x, k_x, k_y) = \frac{a}{\ell} \left[\frac{1 - \gamma(\alpha, k_x) \alpha}{\alpha} \right], \quad (21)$$

where $\gamma(\alpha, k_x)$ is a dimensionless function. In what follows we shall consider only the main instability mode, $k_x = \pi a / 2\ell$, which turns out always to be the most unstable one. For this mode, and in the limit $\alpha \rightarrow 0$, the function $\gamma(\alpha, k_x)$ approaches a constant value ≈ 5 .

Substituting the above expression for G into Eqs. (17) and (18) one obtains the dispersion relation for $\lambda(k_x, k_y)$

$$A_1 \lambda^2 + A_2 \lambda + A_3 = 0. \quad (22)$$

Here

$$A_1 = n \gamma \alpha, \quad A_2 = k_x^2 (1 + \tau A_1) + n k_x^2 + A_1 (h \tau - 1),$$

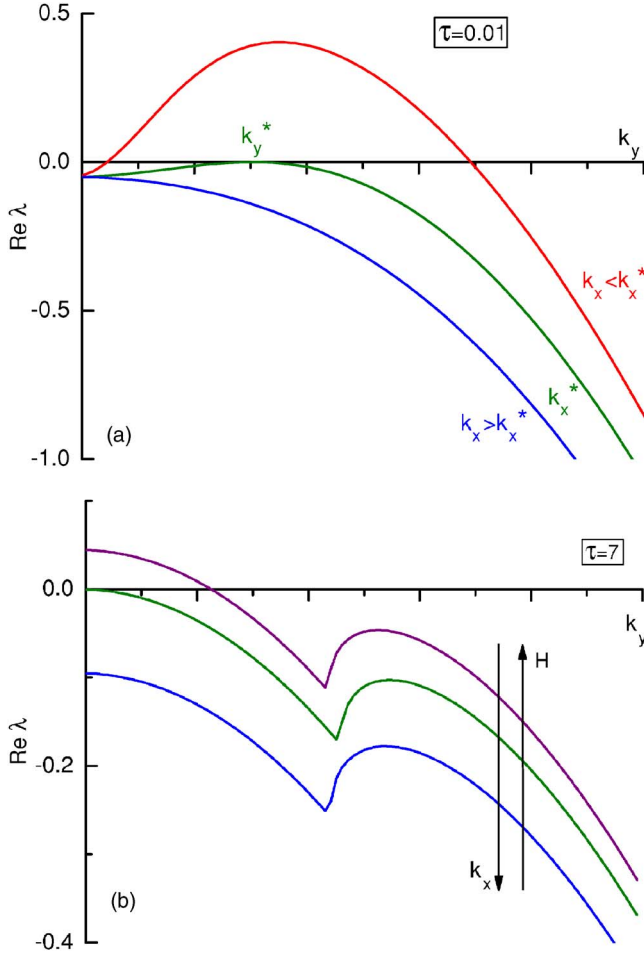


FIG. 2. (Color online) The solutions of dispersion equation (22) for small and large τ , for $\alpha=0.001$ and $n=20$.

$$A_3 = k_y^4 \tau + n k_x^2 k_y^2 \tau + n k_x^2 (h\tau + 1/n) + k_x^2 (h\tau - 1).$$

IV. RESULTS

Let us first consider the simple case of a uniform perturbation, $k_y=0$. One finds from Eq. (22) that the perturbation will grow ($\text{Re } \lambda > 0$) if

$$h\tau < 1 - k_x^2/\gamma\alpha. \quad (23)$$

When the flux penetration region, ℓ , is small, i.e., k_x is large, the system is stable. As the flux advances, k_x decreases, and the system can eventually become unstable. The instability will take place, however, only if $h\tau < 1$. Otherwise the superconducting strip of any width will remain stable no matter how large a magnetic field is applied. This size-independent stability means that at $h\tau \geq 1$ the heat dissipation due to flux motion is slower than heat removal into the substrate.

Equation (23) further simplifies in the adiabatic limit, $\tau \rightarrow 0$, when the heat production is much faster than heat diffusion within the film or into the substrate. The instability then develops at $k_x^2/(\gamma\alpha) < 1$, which in dimensional variables reads as $\mu_0 j_c^2 l d > CT^*(\pi^2/2\gamma)$. Assuming small penetration depth, $l \ll w$, and using Eq. (7) this criterion can be rewritten

as $H > H_{\text{adiab}}$, with the adiabatic instability field

$$H_{\text{adiab}} = \sqrt{\frac{d CT^*}{w \gamma \mu_0}} \sim \sqrt{\frac{d}{w}} H_{\text{adiab}}^{\text{slab}}. \quad (24)$$

Here $H_{\text{adiab}}^{\text{slab}}$ is the adiabatic instability field for the slab geometry.^{1-4,22} This result coincides up to a numerical factor with the adiabatic instability field for a thin strip found recently in Ref. 28.

Solutions of Eq. (22) for perturbations with arbitrary k_y are presented in Fig. 2. The upper panel shows $\text{Re } \lambda(k_y)$ curves for $\tau=0.01$ and different values of k_x . For large k_x , i.e., small magnetic field, $\text{Re } \lambda$ is negative for all k_y . It means that the superconductor is stable. However, at small k_x , the increment $\text{Re } \lambda$ becomes positive in some finite range of k_y . Hence, some perturbations with a spatial structure will start growing. They will have the form of fingers of elevated T and E directed perpendicularly to the flux front. We will call this situation the *fingering (or dendritic) instability*.

For large τ an instability also develops at small k_x , however in a different manner, see Fig. 2 (lower panel). Here the maximal $\text{Re } \lambda$ always corresponds to $k_y=0$. Hence, the uniform perturbation will be dominant. The uniform growth of perturbations for large τ has been recently predicted in Refs. 20 and 21 and explained by the prevailing role of heat diffusion.

Let us now find the critical k_y^* and k_x^* for the fingering instability, see Fig. 2 (upper panel). The k_x^* determines the applied magnetic field when the instability first takes place, while k_y^* determines its spatial scale. These quantities can be found from the requirement $\max\{\text{Re } \lambda(k_y)\}=0$ for $k_y \neq 0$. In the limit $\alpha \ll 1$ we can put $A_1=0$ in Eq. (22) and then rewrite it in the form

$$\lambda = - (k_y^2 + h)\tau + \frac{(k_y^2 - k_x^2)}{k_y^2 + n k_x^2}.$$

From this expression we obtain

$$k_x^* = (\sqrt{n+1} - \sqrt{nh\tau})/n\sqrt{\tau},$$

$$k_y^* = [\sqrt{nh\tau+1}(\sqrt{n+1} - \sqrt{nh\tau+1})]^{1/2}/\sqrt{n\tau}. \quad (25)$$

The dependences of k_x^* , k_y^* on the heat transfer coefficient h are shown in Fig. 3. One can see that k_y^* is always larger than k_x^* implying that fingers of elevated T and E are extended in the direction normal to the film edge. For $h \ll 1/\tau$ and $n \gg 1$ we find $k_y^* \approx n^{1/4} k_x^* \gg k_x^* \approx 1/\sqrt{n\tau}$. Both k_x^* and k_y^* tend to zero as $h \rightarrow 1/\tau$, while for larger h the system is always stable due to fast heat removal to the substrate. It follows from Fig. 2 that for large enough τ the instability will develop uniformly, while for small τ it will acquire a spatially-nonuniform structure. Let us find now the critical value τ_c that separates these two regimes. It can be obtained from the equality $\text{Re } \lambda(k_x=k_x^*, k_y=0)=0$. When it is fulfilled $\text{Re } \lambda=0$ both for $k_y=0$ and for $k_y=k_y^* \neq 0$. We find using Eq. (22) that the instability will evolve in a spatially nonuniform way if

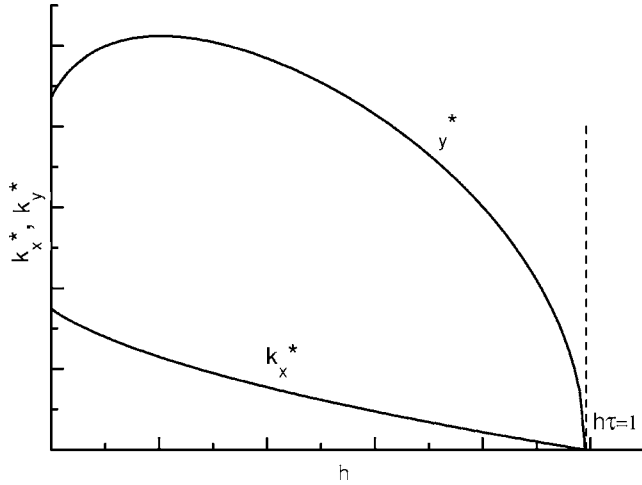


FIG. 3. Dependences of k_y^* and k_x^* on h for $n=20$, $\tau=0.01$, $\alpha=0.001$ according to Eq. (25).

$$\tau < \tau_c = (1 - k_x^{*2}/\gamma\alpha)/h. \quad (26)$$

Substituting here α and k_x^* we find a transcendental relation between τ_c and h . For $n \gg 1$ it reduces to

$$\sqrt{n\tau_c}(1 + \sqrt{h\tau_c}) = \pi a/\gamma d. \quad (27)$$

Using this result we can construct a stability diagram in the E - h_0 plane shown in Fig. 4. The curved line marks the critical electric field $E_c(h_0)$ that separates two types of instability: fingering ($E > E_c$) and uniform ($E < E_c$). This line is calculated from Eq. (27), where the electric field is expressed via τ as $E = j_c \mu_0 \kappa / n C \tau$ according to Eqs. (5) and (6). The straight line is given by the condition $h\tau=1$. Below this line the superconductor is always stable, as follows from Eq. (23) for the uniform perturbations, and from Eq. (25) for the non-uniform case. At a certain value $h_0 = h_{\text{crit}}$, the two lines intercept. We find

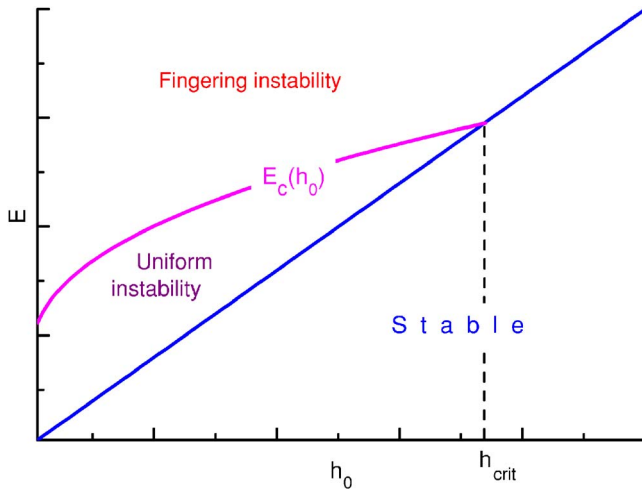


FIG. 4. (Color online) Stability diagram in the plane electric field, heat transfer coefficient according to Eq. (27), and condition $1 - h\tau > 0$ for $n=30$ and $\alpha=0.001$.

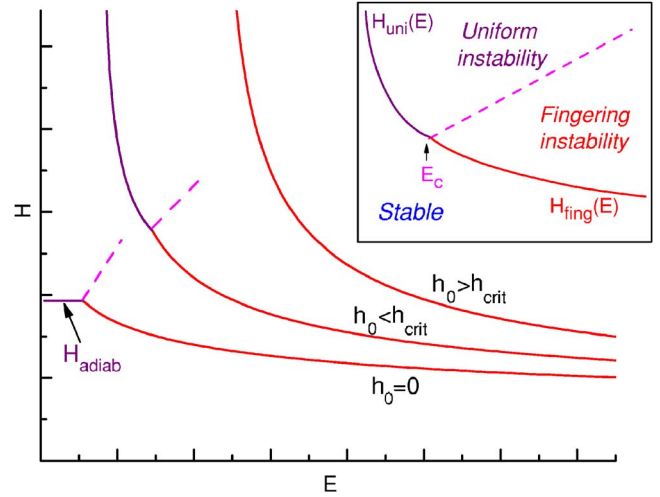


FIG. 5. (Color online) Stability diagram in the H - E plane according to Eqs. (23) and (25).

$$h_{\text{crit}} = \frac{2\gamma^2 \mu_0^2 j_c^4 d^3 \kappa n}{\pi^2 T^{*2} C^2}, \quad (28)$$

and the critical electric field E_c for $h_0=0$ is

$$E_c(0) = \frac{\gamma^2 \mu_0^2 \kappa j_c^3}{\pi^2 C^2 T^{*2}} d^2, \quad (29)$$

while $E_c(h_{\text{crit}}) = 4E_c(0)$.

For any point (h_0, E) belonging to the stable phase in the stability diagram, Fig. 4, the flux distribution is stable for any applied magnetic field. For the points belonging to unstable phases, the instability develops above some threshold magnetic field, either $H_{\text{fing}}(h_0, E)$ or $H_{\text{uni}}(h_0, E)$ for fingering or uniform instability, respectively. Shown in Fig. 5 are three sets of $H_{\text{fing}}(E)$ and $H_{\text{uni}}(E)$ curves for different values of h_0 . They represent boundaries between the three phases, stable and unstable with respect to either fingering or uniform instability, as shown in the inset. Using Eq. (7) one can rewrite the expression (23) for H_{uni} as

$$H_{\text{uni}} = H_{\text{adiab}} \left(1 - \frac{2T^* h_0}{n d j_c E} \right)^{-1/2}. \quad (30)$$

In the absence of heat removal to the substrate, $h_0=0$, we obtain the adiabatic instability field, Eq. (24), and the $H_{\text{uni}}(E)$ curve becomes a horizontal line.²⁹

The threshold magnetic field for the *fingering* instability, H_{fing} , is calculated from Eq. (25). A simplified expression obtained for $h \ll 1/\tau$ and $n \gg 1$

$$H_{\text{fing}} = \left(\frac{j_c d^2}{\pi w} \sqrt{\frac{\kappa T^* j_c}{E}} \right)^{1/2}, \quad (31)$$

shows that at large electric fields H_{fing} decays as $E^{-1/4}$. At $h_0 \leq h_{\text{crit}}$ the curves $H_{\text{fing}}(E)$ and $H_{\text{uni}}(E)$ intercept at the critical electric field E_c determined by Eq. (26). At $h_0 \geq h_{\text{crit}}$ we have $H_{\text{fing}}(E) < H_{\text{uni}}(E)$ for any E , so the lines do not intercept and the instability will develop into a fingering pattern.

V. DISCUSSION

Let us compare the present results for a *thin film* in a perpendicular magnetic field with results of Ref. 20 for a *bulk* superconductor. In both cases the instability develops into a fingering pattern if the background electric field in the superconductor exceeds some critical value E_c . The values of E_c are however different. Their ratio for a thin strip and a slab

$$\frac{E_c(0)}{E_c^{\text{slab}}} = \frac{\gamma^2 d^2 j_c^2 \mu_0}{\pi^2 CT^*}, \quad (32)$$

is expected to be much less than unity. For $j_c = 10^{10}$ A/m², $C = 10^3$ J/Km³, $\kappa = 10^{-2}$ W/Km, $T^* = 10$ K, and $d = 0.3$ μm , we find from Eq. (29) that $E_c \approx 4 \times 10^{-4}$ V/m, while according to Ref. 20, $E_c^{\text{slab}} = 0.1$ V/m. Consequently, the development of thermomagnetic instability into a fingering pattern is much more probable in thin films than in bulk superconductors.

The threshold *magnetic* field for the fingering instability, H_{fing} , is also much smaller for thin films. Comparing Eq. (31) with the results of Ref. 20 for a slab²⁰ we find

$$\frac{H_{\text{fing}}}{H_{\text{inst}}^{\text{slab}}} = \frac{\sqrt{2}}{\pi} \frac{d}{\sqrt{l^*}}. \quad (33)$$

Here $l^* = (\pi/2)\sqrt{\kappa T^*/j_c E}$ is the flux penetration depth at the threshold of the fingering instability, $H = H_{\text{fing}}$. Experimentally, the fingering instability always starts after the flux has penetrated a noticeable distance from the edges, such that $l^* \gg d$.⁵⁻¹⁹ Hence, for a thin film the fingering instability should start at much smaller applied fields than in bulk samples (by a factor of $\sim 10^3$ for films with $d \sim 10^{-4}w$). The difference between the threshold fields for the two geometries here is even stronger than for the case of uniform instability in the adiabatic limit, see Eq. (24). Assuming the above values of parameters and $w = 2$ mm we find from Eq. (31) that $H_{\text{fing}}[E_c(0)] = H_{\text{adiab}} \approx 1$ mT. This value becomes larger if we take into account the heat transfer to the substrate. It is therefore in excellent agreement with the experiment,^{8-10,13,16,17,19,28} where the threshold field is typically of the order of a few mTesla.

The spatial structure of the instability predicted by our linear analysis is a periodic array of fingers perpendicular to the film edge. Its period can be estimated from Eq. (25). For $E = E_c$, $h = 0$ and $n \gg 1$ one finds

$$d_y = \frac{\pi^2 CT^*}{2\gamma n^{1/4} \mu_0 j_c^2 d}, \quad (34)$$

which yields $d_y \approx 100$ μm for $n = 30$. Numerical analysis of the instability development shows^{20,21} that beyond the linear regime the periodic structure is destroyed and only one (strongest) finger invades the Meissner region. This scenario is indeed reproduced experimentally, and the observed width of individual fingers, 20–50 μm ,^{6,8,11,13} is very close to our estimate, $d_y/2$.

The finger width and the threshold magnetic field also depend on the dimensionless parameter h characterizing the thermal coupling to the substrate, Eq. (13). In turn, h , grows

rapidly with temperature because of a strong T dependence of C and j_c . One can therefore make several testable predictions from the dependences $k_x^*(h)$ and $k_y^*(h)$ shown in Fig. 3: (i) There must be a threshold temperature T_{th} above which the instability is not observed. (ii) When approaching T_{th} , the instability field diverges since $k_x^* \rightarrow 0$. (iii) When approaching T_{th} the characteristic width of individual fingers increases since $k_y^* \rightarrow 0$. The last prediction has also been obtained in the boundary layer model allowing calculation of the exact finger shape.³¹ The first and the second predictions have already been confirmed experimentally.^{9,11} As for the last one, the T dependence of the finger width has not yet been studied. At the same time, there is a solid experimental evidence^{8,9,11,19} for an enhanced degree of branching as $T \rightarrow T_{\text{th}}$ that can be quantitatively described as a larger fractal dimension of the flux pattern.¹⁹ This abundant branching could be an indirect consequence of the increased finger width since wider fingers are presumably more likely to undergo splitting.

The present problem of fingering instability in a thin film has two new features compared to a similar problem for a bulk superconductor, (i) nonlocal electrodynamics and (ii) thermal coupling to the substrate. The nonlocality results in much smaller values of the threshold magnetic field H_{fing} and the critical electric field E_c in films than in bulks. If a film is made thinner, it becomes even more unstable since $H_{\text{fing}} \propto d$, and has a stronger tendency to form a fingering pattern since $E_c(0) \propto d^2$. The thermal coupling to the substrate has a somewhat opposite effect. It can lead to an ultimate stability if $h > 1/\tau$, a situation that is never realized in bulks. A moderate coupling, $h \ll 1/\tau$, slightly renormalizes H_{fing} and E_c , i.e., makes the film a little bit more stable and less inclined to fingering.

Let us now compare the results presented in this work to those obtained in a similar model by Aranson *et al.*²¹ Our expressions for the “fingering” threshold field, Eq. (31), and for the finger width, Eq. (34), agree with their results up to a numerical factor. For $\tau \gg 1$ our results for the “uniform” threshold field [derived from Eq. (23)] are also similar to results of Ref. 21. As a new result, we find that there exists a critical value of the parameter τ , Eq. (26), which controls whether the instability evolves either in the uniform, or in the fingering way. Shown in Fig. 4 is the stability diagram where the line $E_c(h_0)$ separates regimes of fingering and uniform instability. Other results of this paper are (i) the existence of a field-independent “critical point,” h_{crit} , such that for $h_0 > h_{\text{crit}}$ the instability *always* develops into a fingering pattern, and (ii) the full stability diagram in the H - E plane, Fig. 5, containing all three phases.

The background electric field needed to nucleate the fingering instability can be induced by ramping the magnetic field, $E \sim \dot{H}l \propto \dot{H}H^2$ for $l \ll w$, where \dot{H} is the ramp rate. This is the lowest estimate since the flux penetration in practice is strongly nonuniform in space and in time,³⁰ and there can be additional sources of E due to random fluctuations of superconducting parameters. The occurrence of the fingering instability even at rather low ramp rates^{5,8-10,13,16-19} is therefore not surprising.

The buildup time of the instability can be estimated as $t_0 \approx 0.1$ μs if the flux-flow conductivity $\sigma = 10^9$ Ω^{-1} m⁻¹. Our

linear analysis assumes that the perturbations of T and E grow in amplitude, but remain localized within the initial flux penetrated region. Numerical results show^{20,21} that at $t \gg t_0$ the perturbations also propagate into the Meissner region. This propagation can be described by recent models^{32,33} that predict a characteristic propagation speed in agreement with experimental values of 10–100 km/s.^{6,7}

In conclusion, the linear analysis of thermal diffusion and Maxwell equations shows that a thermomagnetic instability in a superconducting film may result in either uniform or finger-like distributions of T , E , and B . The fingering distributions will be observed if the background electric field $E > E_c$, where E_c grows with the film thickness, the critical current density, the thermal conductivity and the thermal

coupling to the substrate. Due to nonlocal electrodynamics in thin films they turn out to be more unstable than bulk superconductors and more susceptible to formation of a fingering pattern.

ACKNOWLEDGMENTS

This work is supported by the Norwegian Research Council, Grant No. 158518/431 (NANOMAT), by the U. S. Department of Energy Office of Science through Contract No. W-31-109-ENG-38 and by the Russian Foundation for Basic Research through Project No. 03-02-16626. We are thankful for helpful discussions with V. Vinokur, A. Gurevich, I. Aranson, U. Welp, R. Wijngaarden, and V. Vlasko-Vlasov.

*Electronic address: t.h.johansen@fys.uio.no

¹R. G. Mints and A. L. Rakhmanov, *Rev. Mod. Phys.* **53**, 551 (1981).

²A. V. Gurevich, R. G. Mints, and A. L. Rakhmanov, *The Physics of Composite Superconductors* (Begell House Inc., New York, 1997).

³S. L. Wipf, *Cryogenics* **31**, 936 (1991).

⁴Martin N. Wilson, *Superconducting Magnets* (Clarendon Press, Oxford, 1983).

⁵M. R. Wertheimer and J. de G. Gilchrist, *J. Phys. Chem. Solids* **28**, 2509 (1967).

⁶P. Leiderer, J. Boneberg, P. Brull, V. Bujok, and S. Herminghaus, *Phys. Rev. Lett.* **71**, 2646 (1993).

⁷U. Bolz, B. Biehler, D. Schmidt, B.-U. Runge, and P. Leiderer, *Europhys. Lett.* **64**, 517 (2003).

⁸C. A. Duran, P. L. Gammel, R. E. Miller, and D. J. Bishop, *Phys. Rev. B* **52**, 75 (1995).

⁹M. S. Welling, R. J. Westerwaal, W. Lohstroh, and R. J. Wijngaarden, *Physica C* **411**, 11 (2004).

¹⁰T. H. Johansen, M. Baziljevich, D. V. Shantsev, P. E. Goa, Y. M. Galperin, W. N. Kang, H. J. Kim, E. M. Choi, M.-S. Kim, and S. I. Lee, *Europhys. Lett.* **59**, 599 (2002).

¹¹T. H. Johansen, M. Baziljevich, D. V. Shantsev, P. E. Goa, Y. M. Galperin, W. N. Kang, H. J. Kim, E. M. Choi, M.-S. Kim, and S. I. Lee, *Supercond. Sci. Technol.* **14**, 726 (2001).

¹²A. V. Bobyl, D. V. Shantsev, T. H. Johansen, W. N. Kang, H. J. Kim, E. M. Choi, and S. I. Lee, *Appl. Phys. Lett.* **80**, 4588 (2002).

¹³F. L. Barkov, D. V. Shantsev, T. H. Johansen, P. E. Goa, W. N. Kang, H. J. Kim, E. M. Choi, and S. I. Lee, *Phys. Rev. B* **67**, 064513 (2003).

¹⁴D. V. Shantsev, P. E. Goa, F. L. Barkov, T. H. Johansen, W. N. Kang, and S. I. Lee, *Supercond. Sci. Technol.* **16**, 566 (2003).

¹⁵Zuxin Ye, Qiang Li, G. D. Gu, J. J. Tu, W. N. Kang, Eun-Mi Choi, Hyeong-Jin Kim, and Sung-Ik Lee, *IEEE Trans. Appl. Supercond.* **13**, 3722 (2003).

¹⁶I. A. Rudnev, S. V. Antonenko, D. V. Shantsev, T. H. Johansen,

and A. E. Primenko, *Cryogenics* **43**, 663 (2003).

¹⁷S. C. Wimbush, B. Holzapfel, and Ch. Jooss, *J. Appl. Phys.* **96**, 3589 (2004).

¹⁸M. Menghini, R. J. Wijngaarden, A. V. Silhanek, S. Raedts, and V. V. Moshchalkov, *Phys. Rev. B* **71**, 104506 (2005).

¹⁹I. A. Rudnev, D. V. Shantsev, T. H. Johansen, and A. E. Primenko, *Appl. Phys. Lett.* **87**, 042502 (2005).

²⁰A. L. Rakhmanov, D. V. Shantsev, Y. M. Galperin, and T. H. Johansen, *Phys. Rev. B* **70**, 224502 (2004).

²¹I. S. Aranson, A. Gurevich, M. S. Welling, R. J. Wijngaarden, V. K. Vlasko-Vlasov, V. M. Vinokur, and U. Welp, *Phys. Rev. Lett.* **94**, 037002 (2005).

²²S. L. Wipf, *Phys. Rev.* **161**, 404 (1967).

²³C. P. Bean, *Rev. Mod. Phys.* **36**, 31 (1964).

²⁴E. Zeldov, J. R. Clem, M. McElfresh, and M. Darwin, *Phys. Rev. B* **49**, 9802 (1994).

²⁵E. H. Brandt and M. Indenbom, *Phys. Rev. B* **48**, 12893 (1993).

²⁶W. T. Norris, *J. Phys. D* **3**, 489 (1970).

²⁷A. L. Rakhmanov, D. V. Denisov, D. V. Shantsev, Y. M. Galperin, and T. H. Johansen, *cond-mat/0508679* (2005).

²⁸D. V. Shantsev, A. V. Bobyl, Y. M. Galperin, T. H. Johansen, and S. I. Lee, *Phys. Rev. B* **72**, 024541 (2005).

²⁹Strictly speaking H_{uni} should increase at very small E the same way it does in bulk superconductors (Refs. 1 and 20). This behavior is not reproduced in our model since we neglected the heat flow in the x direction. This flow becomes important only in the limiting case $h_0 \rightarrow 0$. In practice, the heat removal from a thin film to the substrate usually dominates the lateral heat diffusion in the film.

³⁰E. Altshuler and T. H. Johansen, *Rev. Mod. Phys.* **76**, 471 (2004).

³¹C. Baggio, R. E. Goldstein, A. I. Pesci, and W. van Saarloos, *Phys. Rev. B* **72**, 060503(R) (2005).

³²B. Biehler, B.-U. Runge, P. Leiderer, and R. G. Mints, *Phys. Rev. B* **72**, 024532 (2005).

³³B. Rosenstein, B. Ya. Shapiro, and I. Shapiro, *Europhys. Lett.* **70**, 506 (2005).